Comparison of the Parameter Estimation for the Induction Machine Dynamic Model using Instantaneous Measurements at Standstill and during Start-up

José M. Aller*†‡, José A. Restrepo*†‡, Julio C. Viola*†, Pedro R. Barbecho†
Johnny Rengifo‡ and Flavio A. Quizhpi†
*Prometeo - SENESCYT, Quito - Ecuador
†Universidad Politécnica Salesiana, Cuenca - Ecuador
‡Universidad Simón Bolívar, Caracas - Venezuela
email:{jaller, jviola, pbarbecho, fquizhpi}@ups.edu.ec;restrepo@ieee.org; jwrengifo@usb.ve

***Abstract*—This work presents a comparison of three techniques for parameter estimation of the induction machine dynamic model. The first estimation method is based on measurements with the rotor at standstill while several single phase voltage sources are applied at different frequencies. The second method is based on obtaining the instantaneous measurements of voltages and currents during a direct start-up in no load or load condition. To validate the results obtained in each one of these tests, conventional estimation methods are applied to a wound rotor induction machine, according to international standards. The estimation methods are verified using simulations. The obtained results will allow to analyze the accuracy of both methods, and their applicability in industrial environments. The analysis shows the practical conditions where each one of these methods can be applied successfully.**

I. Introduction

For decades, the parameter estimation of the dynamic and static model for induction machines has been a topic of great importance [1], [2], [3], [4], [5]. A proper knowledge of the machine's parameters can be used to adjust angular speed, electric torque or rotor position, by means of scalar or vector controllers [6]. The machine's model also allows the efficiency estimation of its operation and can also be used to diagnose factory defects, misalignments, dynamic or static eccentricities or incipient faults [7], [8].

Several techniques have been developed for parameter estimation of the induction machine. Some of these methods require the use of laboratory facilities with high precision equipment for electrical (voltage, current, power) and mechanical (torque and speed) measurements [9], [10]. Other methods perform the parameter estimation using information from the nameplate and simple electrical tests . It is also possible to estimate parameters when the machine is at standstill [11], by applying controlled voltage sources at different frequencies or by recording the instantaneous measurements of voltages and currents when the electromagnetic drive is in the process of start-up [12].

Each estimation method has different accuracies and scopes, for this reason it is necessary to make a comparison of these methodologies in order to define their specific use. The parameter estimation obtained by tests with rotors at standstill condition, when applying different frequencies to the stator, and those obtained during a start-up of the induction machine (independently of the load condition) will be compared. The basis of comparison between these two methods would be the application of conventional tests according to international standards (stator and rotor resistance measurements, no load test, blocked rotor test, operation at rated power, etc) [13]. All of this work will be applied to a wound rotor induction machine because in this electromagnetic converter the stator and rotor parameters can be determined with a high precision.

Each one of the estimation methods have their own advantages and disadvantages. This work describes the practical conditions for using each method.

II. Dynamic Model of the Induction Machine

A. Coordinate system

There are different coordinate systems (frames), used to describe the behavior of the induction machine. In particular, if the target is the parameter estimation of the induction machine, probably the stator reference frame is the best choice because the instantaneous stator voltages and currents are directly measured.

Even when natural, or primitive coordinates, (a, b, c), represent the simplest induction machine model, the complexity of the expressions obtained in this frame reduce their practical application. Nevertheless, some special conditions such as saturation or internal imbalances, require the use of natural coordinates [14], [15]. The need to transform to uncoupled machine models is critical in obtaining practical interpretation of results, and to perform proper control actions needed by highly dynamic processes. Since the $80's$, the space vector transformation is often used to represent the induction machine dynamic regime [6], [16], [17], because space vectors have the advantage of synthesizing sinusoidal time-varying magnitudes

(voltage, current, linkage fluxes) in a vector whose magnitude and phase vary over time, and uncouple the machine equations. For example,

$$\mathbf{x} \equiv \sqrt{2/3}\left(x_a(t) + x_b(t)\cdot e^{j\frac{2\pi}{3}} + x_c(t)\cdot e^{j\frac{4\pi}{3}}\right) \quad (1)$$

where the coefficient $\sqrt{2/3}$ in (1) is adopted to keep constant the active power in both coordinate systems [16].

B. Space vector model

The induction machine model in space vectors, referred to the stator reference frame can be expressed as,

$$\begin{bmatrix} \mathbf{v}_s \\ \mathbf{v}_r^s \end{bmatrix} = \begin{bmatrix} R_s & 0 \\ 0 & R_r \end{bmatrix}\begin{bmatrix} \mathbf{i}_s \\ \mathbf{i}_r^s \end{bmatrix} + \begin{bmatrix} L_s & M_{sr} \\ M_{sr} & L_r \end{bmatrix} p \begin{bmatrix} \mathbf{i}_s \\ \mathbf{i}_r^s \end{bmatrix} - j\omega \begin{bmatrix} 0 & 0 \\ M_{sr} & L_r \end{bmatrix}\begin{bmatrix} \mathbf{i}_s \\ \mathbf{i}_r^s \end{bmatrix} \quad (2)$$

$$M_{sr}\Im m\left\{\mathbf{i}_s\left(\mathbf{i}_r^s\right)^*\right\} - T_m(\dot{\theta}) = J\,p\omega$$

where:

$$L_s = L_{ls} + \frac{3}{2}L_{ms};\; L_r = L_{lr} + \frac{3}{2}L_{mr},\; M_{sr} = \frac{3}{2}L_{sr}$$

and:

R_s, R_r	Stator and rotor resistances
L_{ls}, L_{lr}	Stator and rotor leakage inductances
L_{ms}, L_{mr}	Stator and rotor magnetizing inductances
L_{sr}	Mutual stator-rotor inductance
p	$\frac{d}{dt}$
$*$	Complex conjugate

C. Reduced parameters model - Γ model

The dynamic induction model expressed in (2) has five parameters (R_s, R_r, L_s, L_r and M_{sr}). A reduced model [6], with only four parameters can be obtained by defining the γ coefficient as as shown in Fig. 1,

$$\gamma \equiv \frac{M_{sr}}{L_r}\,;\; \mathbf{v}_{r\gamma}^s \equiv \gamma\mathbf{v}_r^s\,;\; \mathbf{i}_{r\gamma}^s \equiv \frac{1}{\gamma}\mathbf{i}_r^s \quad (3)$$

then,

$$\begin{bmatrix} \mathbf{v}_s \\ \mathbf{v}_{r\gamma}^s \end{bmatrix} = \begin{bmatrix} R_s & 0 \\ 0 & R_r\gamma^2 \end{bmatrix}\begin{bmatrix} \mathbf{i}_s \\ \mathbf{i}_{r\gamma}^s \end{bmatrix} + + \begin{bmatrix} L_s & M_{sr}\gamma \\ M_{sr}\gamma & M_{sr}\gamma \end{bmatrix} p \begin{bmatrix} \mathbf{i}_s \\ \mathbf{i}_{r\gamma}^s \end{bmatrix} + - j\omega M_{sr}\gamma \begin{bmatrix} 0 & 0 \\ 1 & 1 \end{bmatrix}\begin{bmatrix} \mathbf{i}_s \\ \mathbf{i}_{r\gamma}^s \end{bmatrix} \quad (4)$$

$$M_{sr}\gamma\Im m\left\{\mathbf{i}_s\left(\mathbf{i}_{r\gamma}^s\right)^*\right\} - T_m(\dot{\theta}) = J\,p\omega$$

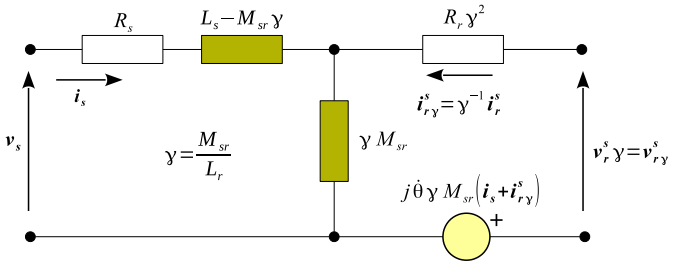

Fig. 1: Reduced parameters, dynamic induction machine model - Γ[11]

III. Parameter Estimation

A. Standstill method

The standstill method, described in [11] is based in the application of voltage sources at several frequencies between two phases of the induction motor. Feeding stator phases a and b of an induction machine, with the rotor at zero speed, results in the steady state equivalent circuit shown in Fig. 2. Peretti's paper [11], considers an induction machine model including saturation effects, but this work deals only with its linear behavior.

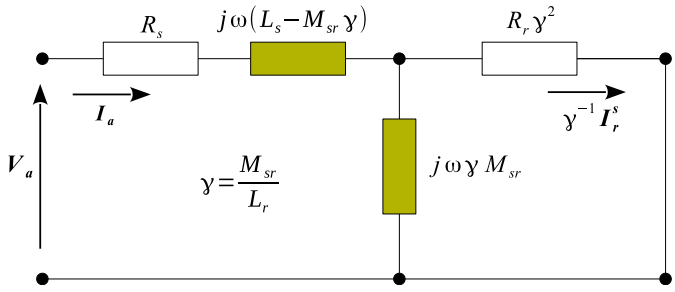

Fig. 2: Steady state induction machine model with reduced parameters, Γ model [11]

By applying a DC voltage source ($\omega = 0$) to the steady state circuit shown in Fig. 2, the resistance R_s is directly obtained as:

$$R_s = \frac{V_{a\,DC}}{I_{a_{DC}}} \quad (5)$$

If a high frequency voltage $V(\omega_h)$ is applied between phases a and b, the input impedance $Z_a(\omega_h)$ is,

$$\mathbf{Z}_a(\omega_h) \approx R_s + R_r\gamma^2 + j\,\omega_h\left(L_s - \gamma M_{sr}\right) \quad (6)$$

where

$$L_s - \gamma M_{sr} = \frac{\Im m\left\{\mathbf{Z}_a(\omega_h)\right\}}{\omega_h} \quad (7)$$

The inductance $L_s - \gamma M_{sr}$ is directly obtained from (6) and (7). The value for $R_r\gamma^2$, in (6), computed using R_s obtained from (5), is at high frequency ω_h, and its value is a bit higher than the real value at low slips. However, this value could be useful during a direct start up.

When a very low frequency ω_l is applied between stator phases a and b, the skin effect in the rotor resistance can be neglected ($\omega_l \approx s_n \omega_{sn}$), and the voltage across $R_r\gamma^2$, is,

$$\mathbf{V}_{R_r\gamma^2} = \mathbf{V}_a - \left[R_s + j\omega_l \left(L_s - \gamma M_{sr}\right)\right] \mathbf{I}_a \tag{8}$$

The rotor resistance $R_r\gamma^2$ is,

$$R_r\gamma^2 = \frac{\left|V_{R_r\gamma^2}\right|^2}{P_{R_r\gamma^2}} = \frac{\left|\mathbf{V}_{R_r\gamma^2}\left(\omega_l\right)\right|^2}{\Re e\left\{\mathbf{V}_{R_r\gamma^2} \cdot \mathbf{I}_a^*\right\}} \tag{9}$$

The rotor resistance $R_r\gamma^2$ obtained from (9) is more precise in the operating range than using (6) because at $\omega_h \gg \omega_{sn}$ the skin effect in rotor conductors affects this parameter, especially when considering double squirrel cage rotor or deep bars.

To estimate γM_{sr}, a DC current $\mathbf{I}_{DC}$ is applied to the stator winding. Before this current reaches a constant value, the stator voltage is short circuited at $t = 0$. Integrating the electromotive force $e_a = v_a\left(t\right) - R_s\, i_a\left(t\right)$, the stator flux linkage λ_a is obtained as,

$$\lambda_a(0) = \int_0^\infty \left(v_a\left(\tau\right) - R_s\, i_a\left(\tau\right)\right) d\tau = -R_s \int_0^\infty i_a\left(\tau\right) d\tau \tag{10}$$

Remembering that $\lambda_a(0) = -L_s i_a(0)$, when $i_r = 0$,

$$L_s = \frac{R_s \int_0^\infty i_a\left(\tau\right) d\tau}{i_a(0)} \tag{11}$$

From (7) and (11), γM_{sr} can be obtained as,

$$\gamma M_{sr} = L_s - \left(L_s - \gamma M_{sr}\right) = L_s - \frac{\Im m\left\{\mathbf{Z}_a\left(\omega_h\right)\right\}}{\omega_h} \tag{12}$$

B. Start-up method

The Γ- induction machine model (4) results in the following stator and rotor equations,

$$\mathbf{v}_s = R_s \mathbf{i}_s + L_s p\mathbf{i}_s + \gamma M_{sr} p\mathbf{i}_{r\gamma}^s \tag{13}$$

$$\mathbf{0} = R_r\gamma^2 \mathbf{i}_{r\gamma}^s + \gamma M_{sr}\left(p - j\omega\right)\left(\mathbf{i}_s + \mathbf{i}_{r\gamma}^s\right) \tag{14}$$

The rotor current $\mathbf{i}_{r\gamma}^s$ can be obtained from the stator linkage flux λ_s as,

$$\mathbf{i}_{r\gamma}^s = \frac{\lambda_s - L_s \mathbf{i}_s}{\gamma M_{sr}} \tag{15}$$

Replacing (15) in (13) and (14) the $\mathbf{v}_s$ voltage is,

$$\begin{aligned} \mathbf{v}_s &= \left[R_s + \frac{R_r\gamma^2}{\gamma M_{sr}} - j\omega\left(L_s - \gamma M_{sr}\right)\right] \mathbf{i}_s + \\ &+ \left(L_s - \gamma M_{sr}\right) p\mathbf{i}_s - \left[\frac{R_r\gamma^2}{\gamma M_{sr}} - j\omega\right] \lambda_s \end{aligned} \tag{16}$$

The instantaneous input impedance $\mathbf{z}_{in}$ results from dividing $\mathbf{v}_s$ by $\mathbf{i}_s$,

$$\begin{aligned} \mathbf{z}_{in} &= \left[R_s + \frac{R_r\gamma^2}{\gamma M_{sr}} - j\omega\left(L_s - \gamma M_{sr}\right)\right] + \\ &+ \left(L_s - \gamma M_{sr}\right) \frac{p\mathbf{i}_s}{\mathbf{i}_s} - \left[\frac{R_r\gamma^2}{\gamma M_{sr}} - j\omega\right] \frac{\lambda_s}{\mathbf{i}_s} \end{aligned} \tag{17}$$

Equation (17) can be used to find parameters R_s, $R_r\gamma^2$, γM_{sr} and $\left(L_s - \gamma M_{sr}\right)$, by optimizing the following least square function,

$$\Psi = \frac{1}{N} \sum_{k=1}^{N} \left(\frac{\mathbf{z}_{in}(k) - \mathbf{z}_{in\,meas.}(k)}{\mathbf{z}_{in\,meas.}(k)}\right) \cdot \left(\frac{\mathbf{z}_{in}(k) - \mathbf{z}_{in\,meas.}(k)}{\mathbf{z}_{in\,meas.}(k)}\right)^* \tag{18}$$

where $\mathbf{z}_{in\,meas}(k)$ is the instantaneous input impedance measured during the start-up of the induction machine. A better performance can be achieved when the stator resistance R_s is directly measured and an optimization algorithm with restrictions is used [12].

C. Standard IEEE method [13]

In the IEEE Std. 112-2004 [13] there are four methods for the parameter estimation of the induction machine model in steady state. These methods are based on the classic no load test to estimate the magnetizing circuit and the blocked rotor test to estimate rotor resistance and leakage reactances. The methods in [13] consider several blocked rotor frequencies to improve the results in different operation conditions. Method 1 is used in this work for the parameter estimation of the induction machine model. In this method the blocked rotor test is performed at rated frequency and with a frequency 25% lower than the rated one. The rotor resistance obtained at rated frequency gives a good aproximation for the starting operation, and the low frequency test matches the performance near rated operation.

The blocked-rotor test requires simultaneous readings of voltage and current in all phases, and of power input at several voltage levels. These measurements need to be done near nominal current conditions. Rotor resistance and leakage reactance are obtained using the following equations [13],

$$Q_o = \sqrt{\left(3V_{10}I_{10}\right)^2 - P_0^2} \tag{19}$$

$$Q_L = \sqrt{\left(3V_{1L}I_{1L}\right)^2 - P_L^2} \tag{20}$$

$$X_m = \frac{3V_{10}^2}{Q_0 - 3I_{10}^2 X_1} \times \frac{1}{\left(1 + \frac{X_1}{X_m}\right)^2} \tag{21}$$

$$X_{1L} = \frac{Q_L}{3I_{1L}^2\left[1 + \left(\frac{X_1}{X_2}\right) + \left(\frac{X_1}{X_m}\right)\right]} \times \left[\frac{X_1}{X_2} + \frac{X_1}{X_m}\right] \tag{22}$$

$$X_1 = \frac{f}{f_L} \times X_{1L} \tag{23}$$

where X_1 and X_2 are the leakage reactance of the stator and rotor respectivelly.

The following algorithm is used to solve equations (21) to (23),

1) Solve (21) for X_m, considering a typical value of X_1/X_m and X_1, for example $X_1/X_m \sim 0.0333$ and $X_1 \sim 0.1\,pu$.
2) Solve (22) for X_{1L}, using the value of X_1/X_m considered in the step 1.
3) Solve (23) for X_1
4) Solve (21) for X_m, using the new value for X_1 obtained in step 3 and the ratio of X_1/X_m from (21).
5) Continue to step 1 until the parameters X_m converge to solution.

After the convergence,

$$X_{2L} = \frac{X_{1L}}{\left(\frac{X_1}{X_2}\right)} \tag{24}$$

$$X_2 = \frac{f}{f_L} \times X_{2L} \tag{25}$$

$$R_m = \frac{3V_{10}^2}{P_{core}} \times \frac{1}{\left(1 + \frac{X_1}{X_m}\right)^2} \tag{26}$$

where P_{core} is the total core loss.

Finally, the rotor resistance from the blocked rotor test can be obtained as,

$$R_{2L} = \left(\frac{P_L}{3I_{1L}2} - R_{1L}\right)\left(1 + \frac{X_1}{X_m}\right)^2 - \left(\frac{X_1}{X_2}\right)^2\left(\frac{X_{1L}^2}{R_m}\right) \tag{27}$$

In equations (21) to (27), the coefficients (X_1/X_2) must be obtained from NEMA MG 1-2014 [18] and is 1.0 for motors with design A and D, 0.67 for design B and 0.43 for design C.

Resistances must be referred in any case to the operational temperature using the following relation,

$$\frac{R_{T2}}{R_{T1}} = \frac{C + T_2}{C + T_1} \tag{28}$$

where C is 234.5 for copper alloy and 225 for aluminum windings.

The parameters of the induction machine, derived with IEEE Std 112-2004 [13] can be used to obtain the Γ model shown in Fig. 2.

IV. Results

The methods are compared by simulations, using the parameters for a $3\,HP$, $220\,V$ @ $60\,Hz$, $1710\,rpm$ induction motor [19]. The parameters estimated for this machine are shown in Table I. The induction machine parameters were obtained using the three methods described in section III.

TABLE I: Parameters of the induction machine for simulation

R_s (Ω)	R_r (Ω)	$L_s = L_r$ (H)	L_m (H)	D Nms	J kgm^2
.435	.816	.0713	.0693	.008	.089
In per unit					
.0201	.0377	1.2424	1.2076	.1271	266.46

A. Estimation at standstill condition

A voltage behind reactance model of the induction machine [20] was implemented in MATLAB-SIMULINK®. This model can evaluate the machine variables at any operational condition (standstill, imbalance and using a voltage source with frequencies in the range from DC to high frequency). Fig. 3 shows parts of the SIMULINK diagram for modeling the induction machine. The MATLAB function fcn, in 3b, is a script with the induction machine equations required by the voltage behind reactance model.

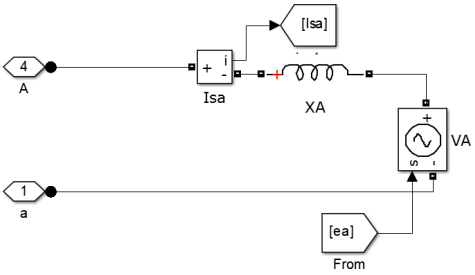

(a) Simulation of each induction machine winding

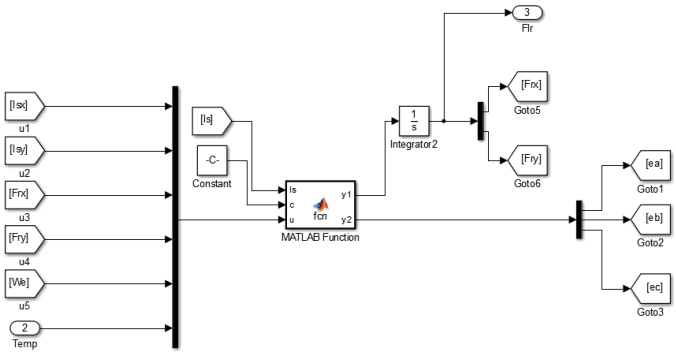

(b) Evaluation of the induction machine model

Fig. 3: Voltage behind reactance SIMULINK® model

B. Estimation using optimization

Dynamic simulations were done using these machine parameters obtained by the estimation methods considered in this paper. Fig. 4 shows the data obtained during a start-up of the induction machine using the parameters given in Table I.

A simulation of the direct start up of the induction machine generates the data used by the optimization algorithm. This optimization assumes knowledge of the stator resistance R_s, and the parameters obtained with this method are shown in Table II. The algorithm was restricted using upper and lower bounds: $0.005 < R_r < 0.1$, $1.0 < M_{sr} < 3.5$, $1.01 < L_e, L_r < 3.7$. The start-up was simulated in the

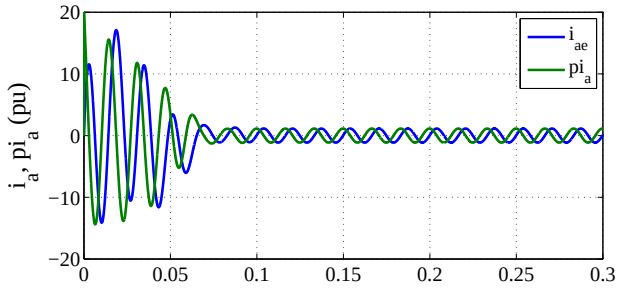

(a) Current i_a and its derivative pi_a during the start-up

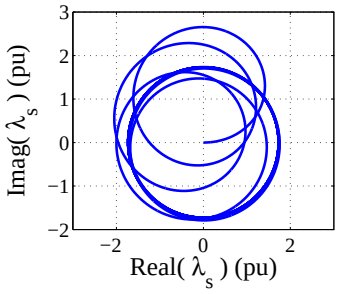

(b) Stator flux linkage λ_s

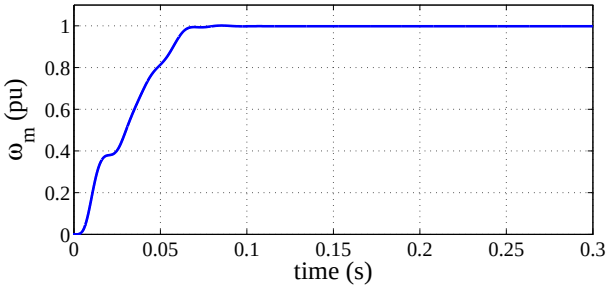

(c) Rotor angular speed ω_m in pu

Fig. 4: Simulating data obtained using parameters given in Table I

no load condition, considering mechanical losses. The total impedance error Ψ obtained using 3000 data points was 1.5717×10^{-7} in 59 iterations, during $1.3\,s$, using function $fmincon$ with the $interior - point$ optimization algorithm available in MATLAB®(2013).

C. Results using IEEE-Std 112(2004)

The results obtained using IEEE-Std 112 are shown in Table II and considers $L_s = L_r$, with direct measurement of the stator resistance R_s and a per unit convergence error below 1×10^{-6}. The error function is $\Psi = (X_m(n) - X_m(n-1))^2 + (X_s(n) - X_s(n-1))^2$.

V. Conclusion

Three estimation methods of the induction machine were compared in this paper. The standstill method is based on applying high and low frequencies as well as DC between two stator phases. The second method uses a start-up of the induction machine, at any-load, and the parameters are obtained with a non linear optimization using the dynamic space vector model. The last one is the conventional IEEE Std. 112, based on no load and blocked rotor test. The error obtained using detailed simulations and the dynamic model of the induction machine are below 1%, for the analyzed methods.

TABLE II: Results obtained with the different estimation methods analyzed

Method	R_s	R_r	L_s	L_r	L_m
Standstill	.0201	0.377	1.2311	1.2311	1.1963
	0	0%	−.9088%	−.9088%	.9485%
Optimization	.0201*	0.0377	1.2392	1.2461	1.2061
	0	0%	−.2576%	.0241%	−.0828%
IEEE Std.112	.0201*	0.377	1.2429	1.2429	1.2071
	0	0%	.0402%	.0402%	0%

* Value obtained by direct measurements

Each method has advantages and disadvantages. The IEEE Std. 112 method requires a complete laboratory facility to be performed, especially if low frequencies are used to improve the rotor resistance estimation. The optimization procedure is easy to implement in an industrial environment and is non intrusive. The standstill method is practical for machines with programmable power electronics drives because the need to feed the machine at rest with a single phase source at different frequencies.

The best method for efficiency determination and predictive maintenance in industrial environments is the parameters optimization during start-up. For robust controllers of the induction machine, the standstill method is very easy to perform before the start-up. IEEE Std. 112 is recommended for use on machine factories, prototypes evaluation or research in machine design.

At present, the authors are working in the experimental validation of the results obtained with the parameter estimation using the dynamic model of the induction machine.

Acknowledgment

The authors gratefully acknowledge the support of Prometeo Project, Secretaría de Educación Superior, Ciencia, Tecnología e Innovación, and Universidad Politécnica Salesiana, both in República del Ecuador, as well as Universidad Simón Bolívar and FONACIT Research Project #2011000970 both in Venezuela.

References

[1] E. Olin, "Determination of power efficiency of rotating electric machines: Summation of losses versus input-output tests," *American Institute of Electrical Engineers, Proceedings of the*, vol. 31, pp. 1287–1310, July 1912.

[2] A. Bellini, A. De Carli, and M. La Cava, "Parameter identification for induction motor simulation," *Automatica*, vol. 12, no. 4, pp. 383–386, 1976.

[3] R. Kerkman, J. D. Thunes, T. Rowan, and D. Schlegel, "A frequency-based determination of transient inductance and rotor resistance for field commissioning purposes," *Industry Applications, IEEE Transactions on*, vol. 32, pp. 577–584, May 1996.

[4] H. Khang and A. Arkkio, "Parameter estimation for a deep-bar induction motor," *Electric Power Applications, IET*, vol. 6, pp. 133–142, February 2012.

[5] X. Zhou, H. Cheng, and P. Ju, "The third-order induction motor parameter estimation using an adaptive genetic algorithm," in *Intelligent Control and Automation, 2002. Proceedings of the 4th World Congress on*, vol. 2, pp. 1480–1484 vol.2, 2002.

[6] A. M. Trzynadlowski, *Control of induction motors*. Academic Pr, 2001.

[7] B. Lu, T. Habetler, and R. Harley, "A survey of efficiency-estimation methods for in-service induction motors," *Industry Applications, IEEE Transactions on*, vol. 42, pp. 924–933, July 2006.

[8] B. Lu, W. Cao, I. French, K. Bradley, and T. Habetler, "Non-intrusive efficiency determination of in-service induction motors using genetic algorithm and air-gap torque methods," in *Industry Applications Conference, 2007. 42nd IAS Annual Meeting. Conference Record of the 2007 IEEE*, pp. 1186–1192, Sept 2007.

[9] E. Agamloh, "A comparison of direct and indirect measurement of induction motor efficiency," in *Electric Machines and Drives Conference, 2009. IEMDC '09. IEEE International*, pp. 36–42, May 2009.

[10] A. de Almeida, F. J. T. E. Ferreira, J. Busch, and P. Angers, "Comparative analysis of ieee 112-b and iec 34-2 efficiency testing standards using stray load losses in low-voltage three-phase, cage induction motors," *Industry Applications, IEEE Transactions on*, vol. 38, pp. 608–614, Mar 2002.

[11] L. Peretti and M. Zigliotto, "Automatic procedure for induction motor parameter estimation at standstill," *Electric Power Applications, IET*, vol. 6, pp. 214–224, April 2012.

[12] J. Rengifo, J. Aller, A. Bueno, J. Viola, and J. Restrepo, "Parameter estimation method for induction machines using the instantaneous impedance during a dynamic start-up," in *Andean Region International Conference (ANDESCON), 2012 VI*, pp. 11–14, Nov 2012.

[13] "IEEE standard test procedure for polyphase induction motors and generators," *IEEE Std 112-2004 (Revision of IEEE Std 112-1996)*, pp. i–, 2004.

[14] S. Pekarek, E. Walters, and B. Kuhn, "An efficient and accurate method of representing magnetic saturation in physical-variable models of synchronous machines," *Energy Conversion, IEEE Transactions on*, vol. 14, pp. 72–79, Mar 1999.

[15] J. Aller, D. Delgado, A. Bueno, J. Viola, and J. Restrepo, "Model of the induction machine including saturation," in *Power Electronics and Applications (EPE), 2013 15th European Conference on*, pp. 1–8, Sept 2013.

[16] J. Aller, A. Bueno, and T. Paga, "Power system analysis using space-vector transformation," *Power Systems, IEEE Transactions on*, vol. 17, pp. 957–965, Nov 2002.

[17] J. M. Aller, *Máquinas eléctricas rotativas: Introducción a la teoría general*. Universidad Simón Bolívar, 2008.

[18] NEMA, "Nema mg 1-2014 motors and generators," *National Electrical Manufacturers Association*, 2014.

[19] J. Cathey, R. Cavin, and A. Ayoub, "Transient load model of an induction motor," *Power Apparatus and Systems, IEEE Transactions on*, vol. PAS-92, pp. 1399–1406, July 1973.

[20] L. Wang, J. Jatskevich, and S. Pekarek, "Modeling of induction machines using a voltage-behind-reactance formulation," *Energy Conversion, IEEE Transactions on*, vol. 23, pp. 382–392, June 2008.